Toughening characterization in alumina platelet–hydroxyapatite matrix composites

S. GAUTIER, E. CHAMPION, D. BERNACHE-ASSOLLANT
Laboratoire de Matériaux Céramiques et Traitements de Surface, UPRESA CNRS 6015, 123, avenue Albert Thomas, 87060 Limoges Cedex, France

Fracture toughness of Al_2O_3 platelet-reinforced hydroxyapatite (HAP) ceramics was investigated using the Vickers' indentation technique. The geometrical anisotropy of alumina platelets induces an anisotropic toughening. The efficiency of reinforcing mechanisms remains maximum for a crack propagating with an angular deviation inferior to 30° around the direction perpendicular to alumina disc faces. This is assumed to result from a crack deflection mechanism which induces a favorable contribution of mode II failure. A small effect of hydroxyapatite grain size becomes noticeable in the direction parallel to alumina disc faces. The toughening depends on the size and volume content of alumina platelets. Large size platelets provoke a spontaneous microcracking of the HAP matrix which is detrimental to the mechanical reliability, whereas small platelets lead to a strong toughening. The results relate to the intensity of thermoelastic residual stresses within the matrix around alumina inclusions.

1. Introduction

During the last decades, numerous synthesized materials, either metals, polymers or ceramics, have been developed for the repair of damaged hard tissues of the human body. Because of a high fracture strength associated with a high fracture toughness, metals such as titanium alloys are now commonly used for prosthetic applications [1, 2]. Ceramic materials can constitute an attractive alternative to metals because their chemical composition may give rise to a better biocompatibility [3, 4]. Among these bioceramics, particular attention has been given to compounds of calcium phosphates whose chemical composition is close to that of the mineral bone [5–7]. Thus, tricalcium phosphate $Ca_3(PO_4)_2$ (TCP), which is soluble in the physiological environment, can be used as temporary implant to enhance bone regeneration. Similarly, hydroxyapatite $Ca_{10}(PO_4)_6(OH)_2$ (HAP), which is able to form a bioactive fixation with the surrounding bone tissues, has become a material of prime interest for permanent implants. The main restriction to the osseo-implantation of ceramics and more particularly of hydroxyapatite derives from a brittle behavior associated with low fracture toughness under mechanical loads (K_{Ic} HAP $\approx 1\,MPa\,m^{1/2}$) [8–13].

The incorporation of a ceramic second phase is known to be a way to improve the mechanical reliability of ceramic matrices [14]. In this field, the reinforcement of polycrystalline ceramics to develop composite materials for high performance applications has been widely reported ($Si_3N_4/SiC_{whisker}$, Al_2O_3/SiC_w, $Al_2O_3/ZrO_{2particle...}$) [15, 16], but few studies have been devoted to the reinforcement of hydroxyapatite matrices. Only some works, concerning the dispersion of zirconia particles, silicon carbide platelets, alumina particles and more recently of hydroxyapatite whiskers, are available [17–24]. In a previous paper devoted to the elaboration and characterization of hydroxyapatite matrix composites, we have demonstrated that the introduction of alumina platelets may provoke a strong toughening [25].

Theoretical models to describe the elementary mechanisms of energy dissipation induced by the incorporation of particles, whiskers or platelets have been established [26–29]. But, because of the combination of several elementary mechanisms and to the influence of physical, chemical or microstructural parameters, any quantitative prediction of the relative gain of toughness which might be expected in a composite system remains often uncertain [30, 31]. On these bases, the present work is concerned with the analysis of the influence of the microstructural design on the toughening in Al_2O_3 platelet/hydroxyapatite matrix composites. It consisted in determining the effect of alumina platelet size, volume fraction and orientation on the toughness increment in relation with a qualitative approach of residual stresses resulting from cooling to room temperature after hot pressing. The influence of the hydroxyapatite grain size was also investigated.

2. Experimental procedure

A commercial hydroxyapatite powder (Bioland, France) was used in this study. This powder had a stoichiometric atomic ratio Ca/P = 1.667 and a specific surface area of $21.2 \pm 0.2\,m^2\,g^{-1}$ (Brunauer–Emmett–Teller; BET method, 8 points–surface analyser Micromeritics ASAP-2010). Alumina platelets (Elf Atochem, France)

TABLE I Main characteristics of Al_2O_3 platelets

Al_2O_3	Average diameter* ø (μm)	Average thickness* h (μm)	Aspect ratio* ø/h	Specific surface area S_s ($m^2 g^{-1}$)
grade T′0	3–7	0.6	5–12	0.83 ± 0.04
grade T2	10–15	1.0	10–15	0.48 ± 0.02

*Supplier data.

were single crystals of corundum phase (α-Al_2O_3). Two grades of platelets were used, corresponding to small and large size platelets and referred as T′0 and T2, respectively. The main characteristics of these grades of alumina are listed in Table I.

Composite mixtures, containing up to 30 vol % of alumina, were homogenized in water with ammonium polymethacrylate as dispersant and ball-milled during 5 h. The suspensions were cast in plaster molds to produce cylindrical compacts. The green composite bodies were dried for 24 h at 40 °C. Then, they were hot pressed in an argon atmosphere at a temperature ranging from 1100 to 1250 °C for 30 min to 4 h under a constant compressive stress of 10 MPa. The thermal treatments were chosen to obtain nearly fully dense composites with varying average grain size of the HAP matrix. Complementary details concerning the elaboration process of these composites can be found elsewhere [25]. Scanning electron microscopy (SEM, Philips XL30) was used for the microstructural observations. The average grain size of the HAP matrix was estimated from SEM micrographs of chemically etched surfaces (lactic acid 0.15 M).

Fracture toughness of the materials was determined, using Vickers' indentation technique (Durometer Zwick 3212), from the measurement of the length of generated surface radial cracks. The samples were mirror polished and the indentation load (P) was applied during 3 s. A 5 N load was used for monolithic HAP and a 39–78 N load was used for the composite materials. K_{Ic} values were calculated from the formula proposed by Evans and Charles [32]

$$\frac{K_{Ic}\Phi}{H_v a^{1/2}} = 0.15k\left(\frac{c}{a}\right)^{-3/2}$$

In this equation, K_{Ic}, a, c and H_v represent the fracture toughness, the indent radius, the radial crack length and the Vickers' hardness, respectively. Φ and k are experimental constants. According to the values of these constants (i.e. $\Phi = 2.7$, $k = 3.2$) and to the definition of the Vickers' hardness, the above-mentioned relation can be simplified and written as follows

$$K_{Ic} = 0.0824Pc^{-3/2}$$

A minimum of height measurements were made for each result point.

Because of a preferred orientation of alumina platelets induced by the processing route, the mechanical characteristics varied with the measurement direction. In order to quantify the effect of the microstructural anisotropy resulting from platelet orientation and to evaluate the influence of the disc-shaped morphology on the toughening, the resistance to crack propagation has been measured in different directions. These directions were referred by the angle θ between the direction defined by the axis of alumina disks and the main direction of the propagating crack plane, as schematized in Fig. 1.

3. Results and discussion

3.1. Influence of the indentation load

The fracture toughness of composites was determined for varying crack lengths. To produce these cracks, the indentation load ranged between 39 and 78 N. Fig. 2 gives the development of fracture toughness versus applied load for composites containing T′0 alumina platelets. The measured crack length varied from 170 μm up to 340 μm in composites containing 10 vol % of platelets, from 120 to 290 μm at 20 vol % and from 120 to 280 μm at 30 vol %. No result is given here for

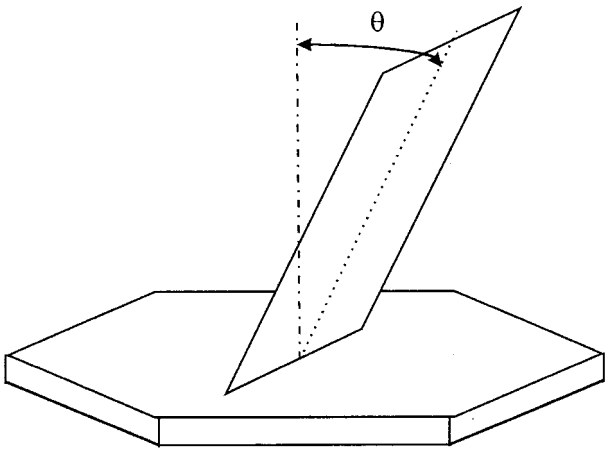

Figure 1 Orientation of crack plane/Al_2O_3 platelet axis.

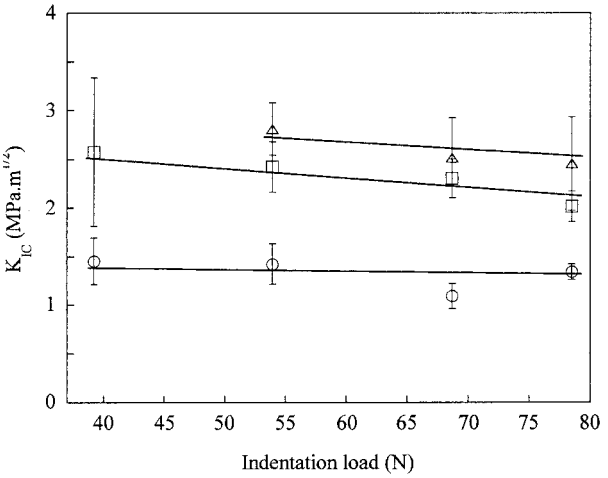

Figure 2 Fracture toughness of composites containing T′0 Al_2O_3 versus Vickers' indentation load; (○) 10 vol % Al_2O_3; (□) 20 vol %; (△) 30 vol %.

composites containing T2 platelets because of a particular behavior of these materials as it will be exposed in the following subsections.

For ceramic materials, the fracture toughness may remain constant or may increase up to a steady-state value with increasing crack length which corresponds to a R-curve behavior [33]. The phenomenon of R-curve, which allows the improvement of the resistance to crack propagation, is commonly described through the development of an active process zone around the crack tip. Though it is sometimes present in monolithic polycrystalline ceramics, this behavior is more generally expected to occur in composite materials because of the ability to develop energy dissipative mechanisms in the wake of the crack tip such as crack bridging or reinforcement pullout.

For HAP-Al_2O_3 composites, no rising fracture toughness with increasing load (i.e. increasing crack length) was observed, K_{Ic} remained always quasi-constant. This does not mean that an R-curve behavior must be excluded but that the steady-state would have been reached. Indeed, this behavior might become effective for shorter cracks in the case of the existence of an active process zone in the wake of the crack tip whose length would be inferior to that of the cracks produced in this experiment. As indicated in a previous paper, crack bridging and platelet debonding occur behind the crack front during crack propagation in HAP-Al_2O_3 composite materials [34]. Consequently, according to the current experiment, the length of the active process zone associated to these mechanisms cannot be superior to about 100 μm. This result agrees with the recent models indicating that the length of a bridging zone hardly exceeds a few tens of microns in platelet-reinforced composites, depending on the thickness, aspect ratio and volume fraction of platelets [31]. In any case, it can be assessed that, in the range of indentation load investigated, all the composites behave identically. Consequently, K_{Ic} measured on the different grades of composites can be directly used to compare the performances of these materials since all these values include the totality of the reinforcing phenomena which might occur. Thus, for the results given in the following sections, the fracture toughness of composites has been determined from a constant indentation load fixed at 54 N.

3.2. Influence of the size and volume content of alumina platelets

Fig. 3 gives the toughness increment induced by the incorporation of alumina platelets with regard to the value of the monolithic HAP matrix which was $K_{Ic\ Matrix} = 0.7 \pm 0.2\ MPa\,m^{1/2}$

$$\Delta K_{Ic} = K_{Ic\ Composite} - K_{Ic\ Matrix}$$

As it will be seen in a following subsection, some variations in the measured toughness may be induced by a change of average grain size of the HAP matrix so that the value given for each point in Fig. 3 must be taken as an average for a composite composition.

For composites containing large alumina platelets

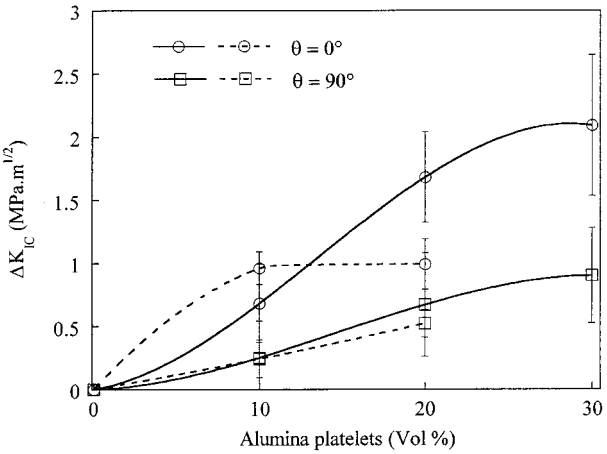

Figure 3 Fracture toughness increment in composites: (—) Al_2O_3 T′0; (- - -) Al_2O_3 T2.

(T2), the fracture toughness increased up to 10 vol % of added alumina with an increment similar to the one obtained when small platelets were used. The maximum gain was close to 1 MPa $m^{1/2}$. Then, for a higher volume fraction of alumina, the increment remained almost constant. No value has been given at 30 vol % of alumina because of too great a discrepancy in the measured values. Thus, the use of platelets of a large size led to a low toughening. Comparing these results with literature data, these composites are not tougher than HAP matrix composites containing spherical alumina particles for which a fracture toughness of 2 MPa $m^{1/2}$ to 2.5 MPa $m^{1/2}$ was found [21]. Therefore, the disc-shaped particles may be no more efficient than spherical ones to develop energy dissipative mechanisms. This could be somewhat controversial because theoretical analyses indicate a superiority of disc-shaped inclusions over spherical particles to develop crack deflection and crack bridging. Consequently, a higher toughening potential would have been expected with the use of platelets.

The incorporation of platelets of a smaller size led to very different results (T′0). The toughness increment increased as the volume fraction of alumina was increased up to 30 vol %. The absolute gain is at least $\Delta K_{Ic} = 1$ MPa $m^{1/2}$ and can reach 2 MPa $m^{1/2}$ at 30 vol % of alumina content, depending on the measurement direction. Compared with the average value measured on dense monolithic hydroxyapatite ($K_{Ic} = 0.7$ MPa $m^{1/2}$) these toughness increments show the efficiency of small alumina discs to improve the mechanical reliability of HAP-based materials. But, a strong anisotropy of the mechanical characteristic is observed in association with the preferred orientation of platelets.

In the light of these results, the size of the disc-shaped inclusions is of prime importance for the mechanical reliability of composites. SEM observations of composite surfaces allowed to confirm the influence of this parameter. Typical microstructures of materials containing 20 vol % of Al_2O_3 of grade T′0 and T2 are given in Figs 4 and 5, respectively. They show the presence of numerous intergranular microcracks within the HAP matrix when large platelets were used whereas no matrix microcracking was observed with the incorporation of small platelets.

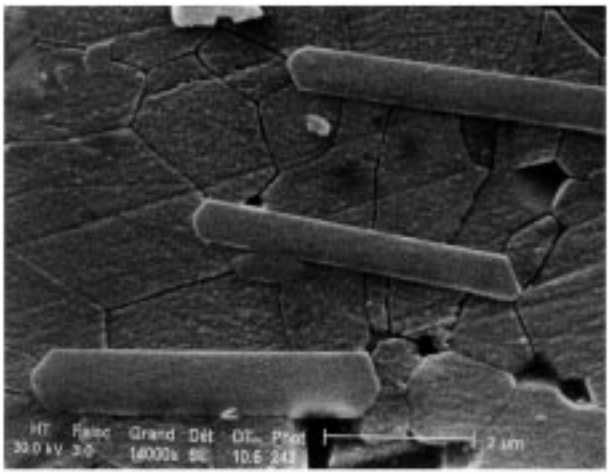

Figure 4 SEM micrograph of HAP-20 vol% Al_2O_3 T′0 composite (H. P. 1200 °C, 2 h).

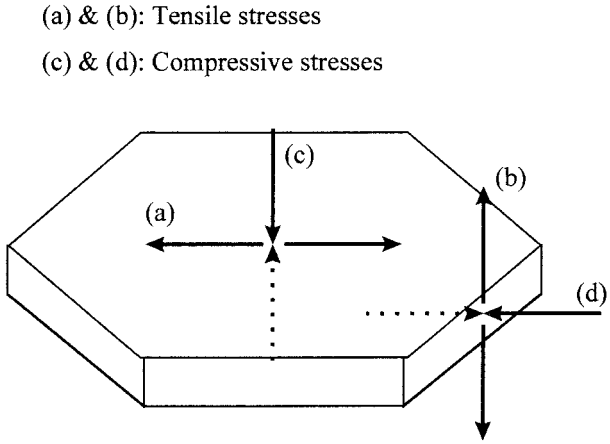

Figure 6 Schematic of residual stresses within the HAP matrix around an Al_2O_3 platelet.

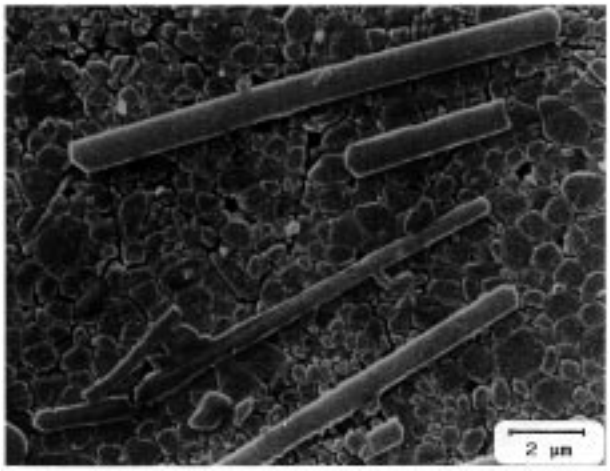

Figure 5 SEM micrograph of HAP-20 vol% Al_2O_3 T2 composite (H. P. 1200 °C, 30 min).

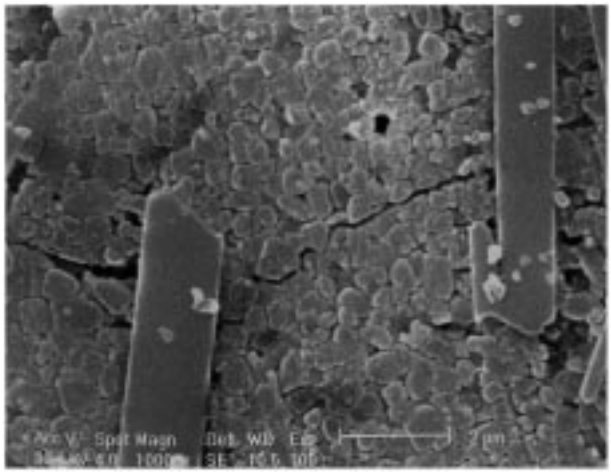

Figure 7 SEM micrograph of HAP-20 vol % Al_2O_3 T2 composite: extent of microcracks within the matrix.

It can be assessed that the creation of microcracks in the matrix results from residual stresses developed during cooling at room temperature after thermal treatment of densification. These residual thermoelastic stresses have been analyzed by Li and Bradt [35]. For a disc-shaped inclusion having a thermal expansion coefficient inferior to the one of the matrix, which is the case of HAP-Al_2O_3 composites ($\alpha_{HAP} \approx 16.10^{-6}$ K^{-1}; $\alpha_{Alumina} \approx 8.10^{-6} K^{-1}$), tangential tensile stresses and radial compressive stresses appear in the matrix just outside of the inclusion, as schematized in Fig. 6 [36]. The stresses inside the inclusion are compressive. The intensity of these residual stresses increases as the aspect ratio Φ/h of discs increases and/or when the volume fraction of inclusions is increased.

The experimental results agree with this analysis. The presence of tensile residual stresses within the HAP matrix may be responsible for the low mechanical reliability registered in composites containing from 20 vol % of large alumina platelets. The increase of the aspect ratio (Φ/h) of Al_2O_3 discs, associated to the change of platelet grade from T′0 to T2, increases the intensity of tensile stresses within the HAP matrix which could have provoked the observed microcracks (Figs 5 and 7). In the same way, the increase of alumina volume content could then lead to the spontaneous extension of these microcracks to form a network in the whole matrix. The presence of cracks also explains the restricted toughness increment measured for composites containing T2 alumina and the too low accuracy of results obtained for materials containing 30 vol % of these platelets.

But, it is also known that, providing the initial microcracks remain small enough and localized, the microcracking of a composite matrix may contribute to the reinforcement by initiating crack branching [27]. This could be the case in composites containing small platelets in which tensile residual stresses must be less intense than in materials containing large platelets. Though the examination of microstructures has not allowed to confirm clearly this hypothesis, some observations seem to point out the presence of such small microcracks in the HAP matrix around T′0 platelets (arrows on Fig. 8). These microcracks can contribute to crack branching, mechanism already observed in similar composites [34], and therefore to the toughening.

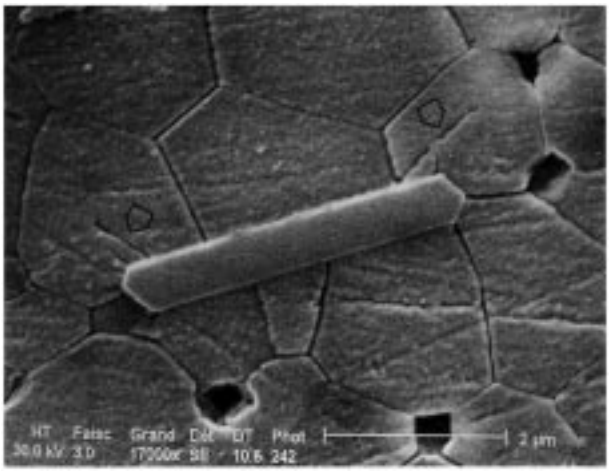

Figure 8 SEM micrograph of HAP-20 vol % Al_2O_3 T′0 composite: initiation of microcracks in the matrix.

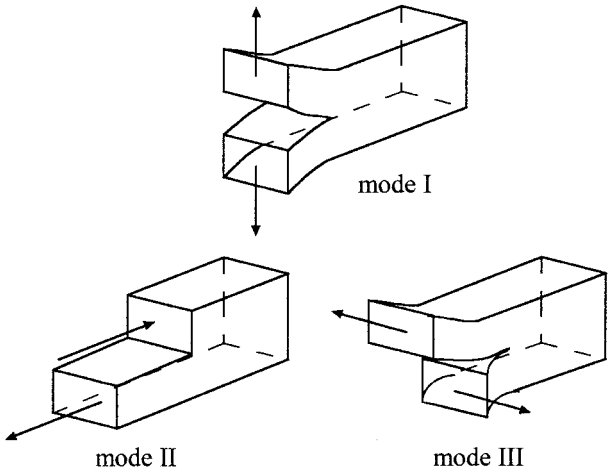

Figure 10 Elementary modes of failure under mechanical load.

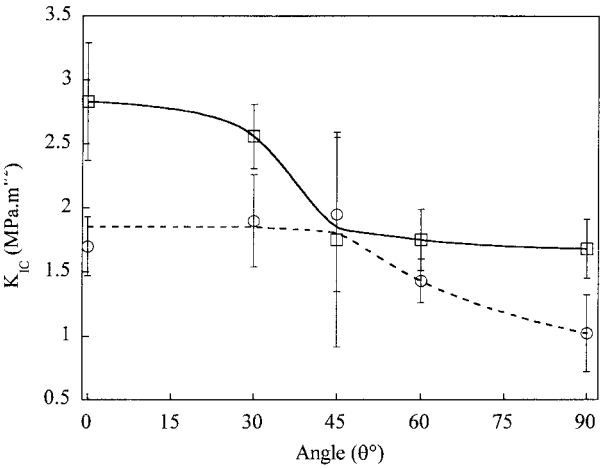

Figure 9 Fracture toughness of composites versus platelet orientation. (○) HAP-10 vol % Al_2O_3 T2; (□) 30 vol % Al_2O_3 T′0.

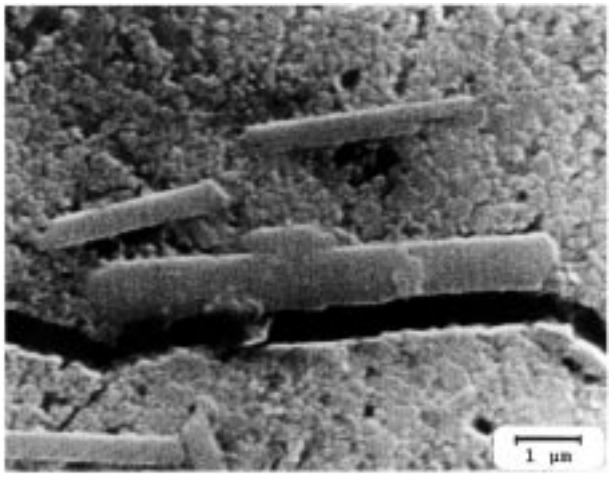

Figure 11 SEM micrograph of a crack propagated in the direction 90°.

3.3. Influence of platelet orientation

This part of the study has been performed using composites containing 30 vol % of T′0 alumina and 10 vol % of T2 alumina. These two compositions were chosen because they lead to the highest toughness registered on materials containing small and large size platelets, respectively. Fig. 9 gives the plots of fracture toughness versus platelet orientation (as defined in Fig. 1).

It can be noted that whatever the orientation of platelets might be, their presence induced a toughening of the material. Similar variations of fracture toughness with the crack plane orientation were obtained independently of platelet size. Compared with the monolithic matrix, the relative gain ranged from a minimum of about 200% to a maximum of about 400% with small platelets. Though it remained more limited with the use of large platelets, it was at least of about 50% and reached a maximum close to 200%.

The phenomena involved in the propagation of a crack and the associated energy dissipative mechanisms can be explained in considering the nature of residual stresses around platelets and the elementary modes of failure (Fig. 10) [37]. The hypothesis is that a crack tends to propagate preferentially in a direction perpendicular to tensile stresses; therefore, in mode I which is recognized as the most critical mode of crack propagation in brittle materials. This corresponds to the behavior of the monolithic HAP matrix.

In HAP-Al_2O_3 composite materials, three different domains of toughening can be distinguished depending on the orientation of the propagating crack:

1. For an angle superior to 60°, the toughness remains at its minimum value. Fig. 11 shows a SEM micrograph of a crack propagated in the direction $\theta = 90°$. The crack has propagated along the platelet face without deflection. And, similarly to the monolithic matrix, the propagation occurs mainly in mode I of failure. Consequently, the toughness increment measured in composites should result from a predominant effect of the residual thermoelastic stresses induced around the alumina platelet. Indeed, in this direction of propagation, tensile stresses developed in the matrix at the edge of a platelet (Fig. 6b) tend to direct the propagating crack front towards the platelet face. Then, when the crack propagates along the platelet face, compressive stresses located along this platelet face (Fig. 6c) reduce the stress intensity at the crack tip and therefore contribute to a toughening effect.

2. For an angle inferior to 30°, the toughness remains at its maximum value. In this domain, a crack tends to propagate in a plane perpendicular to platelet faces and

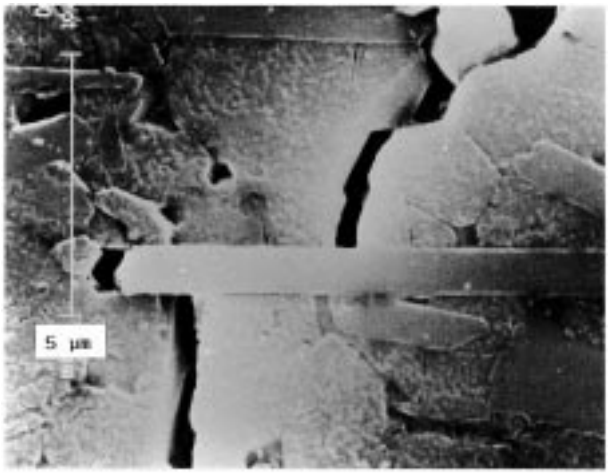

Figure 12 SEM micrograph of a crack propagated in the direction 0°.

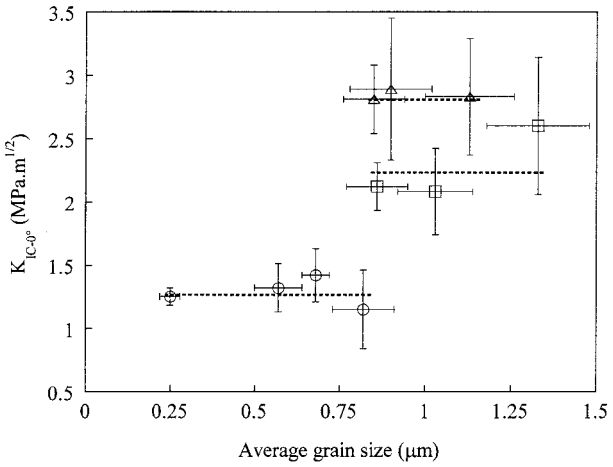

Figure 13 Fracture toughness of composites versus average grain size of HAP ($\theta = 0°$). (○) 10 vol % Al_2O_3; (□) 20 vol %; (△) 30 vol %.

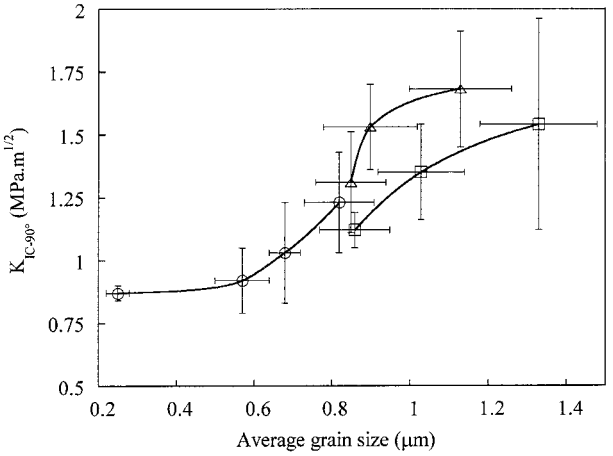

Figure 14 Fracture toughness of composites versus average grain size of HAP ($\theta = 90°$). (○) 10 vol % Al_2O_3; (□) 20 vol %; (△) 30 vol %.

the reinforcement mechanisms occur with the highest efficiency. Fig. 12 shows a typical view of a crack propagated in the direction $\theta = 0°$. Crack deflection along platelet face and platelet debonding can be observed. Around a platelet, the propagation of a crack occurs in a mixed mode of failure, combining mode I and II. The contribution of residual stresses remains similar to that described in (1). Tensile stresses (Fig. 6a) tend to direct the crack front towards the platelet face. Then, compressive stresses (Fig. 6c and d) reduce the stress intensity as the crack propagates along the platelet face. But, conversely to the case (1), the propagation along the platelet face occurs mainly in mode II. Finally, in this direction, a combination of several energy dissipative mechanisms occur which further enhance the resistance of the material to crack propagation: platelet debonding in the crack wake is associated to a deflection of the crack tip on platelet face along which compressive residual stresses combine with mode II of failure. Though there is no evidence for any predominance of one of these mechanisms on the others, it could be hypothesized that the contribution of platelet debonding to the total energy dissipation should remain minor. As shown in Fig. 12, because of the small size of alumina platelets, debonding can be effective and efficient only on a very short length in the order of 1 µm long.

3. Intermediate angles, comprised between 30° and 60°, correspond to the domain of transition between these last two extreme situations.

3.4. Influence of the average grain size of the HAP matrix

Because of the difficulty to elaborate reliable composites with platelets of the largest size, the investigation on the effect of average grain size of the hydroxyapatite matrix has been restricted to materials containing small alumina platelets. Figs 13 and 14 give the fracture toughness of these composites determined in the directions $\theta = 0°$ and $\theta = 90°$, respectively. The plots showed that there was no evidence for an influence of the average grain size of the matrix in the direction of highest fracture toughness, K_{Ic} values remaining constant (Fig. 13). Conversely, in the direction of lowest toughness (Fig. 14), the relative influence of the microstructure of the matrix became noticeable. A slight increment of fracture toughness was registered with the increase of the average grain size of HAP. Whatever the volume content of alumina might be, the absolute gain in toughness between the smallest and the largest average grain size was of the order of $\Delta K_{Ic} = 0.3$ MPa m$^{1/2}$. This value can be compared with the average toughness increment resulting in the incorporation of T′0 platelets (in the same direction $\theta = 90°$) which was of about 0.25 MPa m$^{1/2}$, 0.6 MPa m$^{1/2}$ and 0.9 MPa m$^{1/2}$ for 10, 20 and 30 vol % of alumina, respectively (Fig. 3). Thus, it appears that from 20 vol % the contribution of alumina platelets to the toughening becomes preponderant.

These results point out the predominant effect of alumina platelets on the toughness when they are favorably oriented to induce several energy dissipative mechanisms. The relative contribution of HAP grain size becomes significant only when the influence of these mechanisms is reduced to its minimum, that is to say for a low alumina content and in the direction $\theta = 90°$.

Based on literature data, two main phenomena could be taken on account to explain the increase of fracture toughness with increasing grain size of the HAP matrix.

1. Rice and co-workers have demonstrated that the fracture energy of a single phased polycrystalline

ceramic material increases to reach a maximum value for an intermediate grain size and then decreases for a larger grain size [38, 39]. This toughening effect may be associated to a local microcracking mechanism resulting from thermal expansion anisotropy of adjacent crystals [40]. A local microcracking between adjacent grains of HAP induced by grain growth in association with the thermal expansion anisotropy of the HAP crystals can exist because of the important mismatch of thermal expansion coefficients of the hydroxyapatite lattice ($\alpha_{a\,axis} \approx 13.10^{-6}K^{-1}$; $\alpha_{c\,axis} \approx 22.10^{-6}K^{-1}$) [41]. Such microcracks were already observed in a previous study concerning the characterization of the monolithic HAP matrix [12]. Nevertheless, these microcracks have not been observed in composites, the small microcracks which were sometimes present in composites containing small alumina platelets appeared at the Al_2O_3-HAP interfaces (Fig. 8).

2. Buljan *et al*. developed a model indicating that a moderate increase in grain size may induce a small toughness increment [42]. In this case, the toughening could be attributed to an increasing contribution of crack deflection along HAP grain boundaries with increasing grain size.

4. Conclusions

This study demonstrates that the toughening of hydroxyapatite matrices induced by the incorporation of alumina platelets results from the combination of several mechanisms, the efficiency of these mechanisms being meanly governed by two parameters:

1. The thermoelastic residual stresses developed within the HAP matrix just outside of the alumina inclusions during the cooling after the thermal treatment of densification. They result from the thermal expansion mismatch between the HAP and Al_2O_3 phases and depend on the size and volume content of alumina platelets. Radial compressive stresses are in favor with the resistance to crack propagation. However, the intensity of associated tangential tensile stresses must remain low enough to avoid a spontaneous microcracking of the HAP matrix. This is achieved providing the aspect ratio of the Al_2O_3 discs (ϕ/h) does not exceed about 10.

2. The disc-shaped morphology of alumina particles. The geometrical anisotropy of platelets may give rise to crack deflection and impose mode II of failure along platelet faces which is more unfavorable to the propagation than mode I. But, to be really efficient, this particle morphology requires to achieve a preferred orientation of disc faces which must lie in parallel planes with an angular deviation below 30°.

Finally, the reinforcement mechanisms are strongly dependent on the alumina phase, the grain size of the hydroxyapatite matrix having little influence on the mechanical reliability of composites. The choice of both size and shape of alumina inclusions appears of prime importance in the elaboration of toughened hydroxyapatite based composites.

Acknowledgments

The authors would like to thank Bioland for the financial support provided for this research project.

References

1. D. I. BARDOS, in ''Concise encyclopedia of medical & dental materials'', edited by D. Williams (Pergamon Press, Oxford, 1990) p. 360.
2. J. P. MEYRUEIS, in ''Les biomatériaux en chirurgie orthopédique'', edited by J. Duparc (Cahiers d'enseignement de la SOFCOT, Paris, 1986) p. 25.
3. L. L. HENCH, *J. Amer. Ceram. Soc.* **74** (1991) 1487.
4. G. HEIMKE, *Adv. Ceram. Mater.* **2** (1987) 764.
5. K. D. GROOT, in ''Bioceramics of calcium phosphate'', edited by K. D. Groot (CRC Press, Boca Raton, FL, 1983) p. 99.
6. M. JARCHO, *Clin. Orthop. Rel. Res.* **157** (1981) 259.
7. R. W. BUCHOLZ, A. CARLTON and R. E. HOLMES, *Orthop. Clin. N. Amer.* **18** (1987) 323.
8. M. B. THOMAS and R. H. DOREMUS, *Ceram. Bull.* **60** (1981) 258.
9. G. D. WITH, H. J. A. V. DIJK, N. HATTU and K. PRIJS, *J. Mater. Sci.* **16** (1981) 1592.
10. M. AKAO, N. MIURA and H. AOKI, *Yogyo Kyokai Shi* **92** (1984) 78.
11. J. LI and L. HERMANSSON, *Interceram* **39** (1990) 13.
12. R. HALOUANI, D. BERNACHE-ASSOLLANT, E. CHAMPION and A. ABABOU, *J. Mater. Sci.: Mater. Med.* **5** (1994) 563.
13. P. V. LANDUYT, F. LI, J. P. KEUSTERMANS, J. M. STREYDIO, F. DELANNAY and E. MUNTING, *ibid.* **6** (1995) 8.
14. R. W. RICE, *Ceram. Engng. Sci. Proc.* **2** (1981) 661.
15. K. XIA and T. G. LANGDON, *J. Mater. Sci.* **29** (1994) 5219.
16. S. T. BULJAN, A. E. PASTO and H. J. KIM, *Ceram. Bull.* **68** (1989) 387.
17. K. IOKU, M. YOSHIMURA and S. SOMIYA, *Biomaterials* **11** (1990) 57.
18. M. TAKAGI, M. MOCHIDA, N. UCHIDA, K. SAITO and K. UEMATSU, *J. Mater. Sci.: Mater. Med.* **3** (1992) 199.
19. V. S. NAGARAJAN and K. J. RAO, *J. Mater. Chem.* **3** (1993) 43.
20. T. NOMA, N. SHOJI, S. WADA and T. SUZUKI, *J. Ceram. Soc. Jpn* **100** (1992) 1175.
21. *Idem*., *ibid.* **101** (1993) 923.
22. H. JI and P. M. MARQUIS, *J. Mater. Sci.* **28** (1993) 1941.
23. A. J. RUYS, A. BRANDWOOD, B. K. MILTHORPE, M. R. DICKSON, K. A. ZEIGLER and C. C. SORRELL, *J. Mater. Sci.: Mater. Med.* **6** (1995) 297.
24. W. SUCHANEK, M. YASHIMA, M. KAKIHANA and M. YOSHIMURA, *J. Amer. Ceram. Soc.* **80** (1997) 2805.
25. S. GAUTIER, E. CHAMPION and D. BERNACHE-ASSOLLANT, *J. Eur. Ceram. Soc.* **17** (1997) 1361.
26. K. T. FABER and A. G. EVANS, *Acta Metall.* **31** (1983) 565.
27. A. G. EVANS and K. T. FABER, *J. Amer. Ceram. Soc.* **64** (1984) 394.
28. P. F. BECHER, C. H. HSUEH, P. ANGELINI and T. N. TIEGS, *ibid.* **71** (1988) 1050.
29. G. PEZZOTTI, *Acta Metall. Mater.* **41** (1993) 1825.
30. P. F. BECHER, *J. Amer. Ceram. Soc.* **74** (1991) 255.
31. G. PEZZOTTI, Y. OKAMOTO, T. NISHIDA and M. SAKAI, *Acta Mater.* **44** (1996) 899.
32. A. G. EVANS and E. A. CHARLES, *J. Amer. Ceram. Soc.* **59** (1976) 371.
33. S. W. FREIMAN, *Ceram. Bull.* **67** (1988) 392.
34. E. CHAMPION, S. GAUTIER and D. BERNACHE-ASSOLLANT, *J. Mater. Sci.: Mater. Med.* **7** (1996) 125.
35. Z. LI and R. C. BRADT, *J. Amer. Ceram. Soc.* **72** (1989) 70.
36. E. ESPERANCE, Thesis, Ecole Nationale Supérieure des Mines, Saint-Etienne, France, 1992.

37. F. OSTERSTOCK, G. VADAM and J. L. CHERMANT, *Mémoires Scientifiques de la Revue Métallurgie* (1980) 7.
38. R. W. RICE, S. W. FREIMAN and P. F. BECHER, *J. Amer. Ceram. Soc.* **64** (1981) 345.
39. R. W. RICE and S. W. FREIMAN, *ibid.* **64** (1981) 350.
40. Y. FU and A. G. EVANS, *Acta Metall.* **30** (1982) 1619.
41. G. R. FISCHER, P. BARDHAN and J. E. GEIGER, *J. Mater. Sci. Lett.* **2** (1983) 577.
42. S. T. BULJAN, J. G. BALDONI, M. L. HUCKABEE and G. ZILBERSTEIN, in ''Conference Proceedings of ASMI'', edited by R. A. Bradley, D. E. Clark, D. C. Larsen and J. O. Stiegler (ASMI, 1988) p. 113.

Received 30 July
and accepted 28 August 1998